Preparing for Diphoton Resonance Searches in the Leptonic, 0-τ Final States: Event Selection and Background Characterization Using ATLAS Run 3

Kgothatso Ntumbe[1,2], Baballo-Victor Ndhlovu[1,2], Kutlwano Makgetha[1,2], Njokweni Mbuyiswa[1,2], Phuti Rapheeha[1,2,4], Reda Mekouar[3], Thabo Pilusa[1,2], Vuyolwethu Kakancu [1,2], Bruce Mellado[1,2], Mukesh Kumar[1,2], Rachid Mazini[1]

[1] School of Physics and Institute for Collider Particle Physics, University of the Witwatersrand, Johannesburg, Wits 2050, South Africa
[2]iThemba LABS, National Research Foundation, PO Box 722, Somerset West 7129, South Africa
[3]Institute of High Energy Physics, Beijing, University of Chinese Academy of Sciences, 19B Yuquan Road, Shijingshan District, Beijing, China
[4]School of Electrical Engineering, Tshwane University of Technology, Staatsartillerie Road, Pretoria West 0001, South Africa

E-mail: 2445026@students.wits.ac.za

Abstract.

The search for new scalar resonances at the Large Hadron Collider (LHC) is motivated by beyond the Standard Model (BSM) scenarios such as the Two-Higgs-Doublet Model with an additional scalar singlet (2HDM+S) and the Real Higgs Triplet Model. The 2HDM+S and Triplet model BSM frameworks is being used to study new scalar particles that may decay into final states involving photons and leptons. In particular, these models motivate searches for di-photon signatures accompanied by leptons. This study focuses on scalar resonance production via the process $gg \to H \to SS'$, where $S \to \gamma\gamma$, and S' decays into one or more leptons and/or hadrons. Relevant decay modes of S' include τ, $\ell + b$ ($\ell = e, \mu$), and multi-body final states such as 2ℓ, 2τ, or combinations thereof. Among the various final states, particular attention is given to the channels $\gamma\gamma + \ell, 0\tau$ and $\gamma\gamma + 2\ell, 0\tau$, given their sensitivity to scalar resonances and experimental accessibility. We are currently developing analysis strategies and selection tools in preparation for the analysis of ATLAS Run 3, corresponding to $\sqrt{s} = 13.6$ TeV. The goal is to identify signal-like events while mitigating dominant SM backgrounds.

1 INTRODUCTION

The Standard Model (SM) of particle physics offers a remarkably precise description of known fundamental interactions and particles. However, it does not account for several critical phenomena, including the existence of dark matter, the origin of neutrino masses, and the observed matter–antimatter asymmetry in the universe. These open questions strongly motivate the pursuit of physics beyond the Standard Model (BSM). Among the many proposed BSM scenarios, scalar sector extensions such as the Two-Higgs-Doublet Model with an additional singlet scalar (2HDM+S)[1] and the Real Higgs Triplet Model[2] provide compelling theoretical frameworks. These models predict new scalar particles that can decay into diphoton and multilepton final states, which are accessible to experimental searches at the LHC. In the context of this study, Monte Carlo signal samples currently in production are based on the 2HDM+S model.

Both the 2HDM+S and Real Higgs Triplet Model predict the existence of a heavy scalar resonance that decays through processes such as $gg \to H \to SS'$, where one scalar (S) decays to a diphoton final state ($\gamma\gamma$) and the other scalar (S') decays to leptons, two hadronic taus, b-quarks, or multi-body final states as seen in the feynmann diagram (1). Final states such as $\gamma\gamma + 1\ell$ and $\gamma\gamma + 2\ell$ are particularly promising for these searches due to their clean experimental signatures. The diphoton system benefits from excellent energy resolution and low background rates in the ATLAS electromagnetic calorimeter, while the presence of prompt, isolated leptons especially electrons and muons enhances background discrimination. The dominant Standard Model backgrounds considered thus far in these final states arise from processes such as $\gamma\gamma jj$, $t\bar{t}\gamma\gamma$, and $V\gamma\gamma$. These samples are being studied in detail to inform selection optimization, guide background suppression strategies, and validate the overall analysis framework.

This work focuses on the preparation and development of an analysis strategy for BSM scalar resonance searches in the $\gamma\gamma + 1\ell$ and $\gamma\gamma + 2\ell$, 0-τ final states. Rather than using Run 3 data directly, we utilize existing background Monte Carlo samples, with emphasis on the $t\bar{t}\gamma\gamma$ Ntuple, to define and test event selections, object definitions, and calibration tools. These efforts serve to configure and validate the Easyjet framework, which provides a modular and reproducible structure for building the full analysis pipeline. Additional backgrounds relevant to our targeted final states are being studied to refine selection strategies and support future background modeling. At this stage, signal Monte Carlo samples are still in production. As such, the results presented in this document are based entirely on background studies, and are intended to provide a solid foundation for the analysis once signal samples become available. The report that follows describes the motivation, background composition, selection methodology, framework integration, and object-level distributions that underpin this preparatory work.

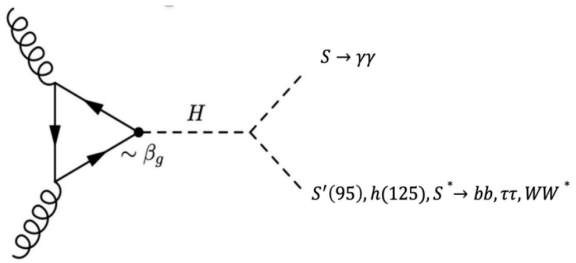

Figure 1: Feynman diagram illustrating the production of a heavy scalar resonance H via gluon-gluon fusion, mediated by a top loop with coupling $\sim \beta_g$. The resonance decays into two lighter scalars: $S \to \gamma\gamma$ and S', where S' can be either a new scalar ($S'(95)$), the SM-like Higgs boson ($h(125)$), or another scalar state. The S' decays into final states such as $b\bar{b}$, $\tau^+\tau^-$, or off-shell W^+W^-, leading to rich experimental signatures[1].

2 Background Characterization

In the absence of signal samples, our current analysis strategy is driven by a detailed study of relevant Standard Model (SM) background processes. These backgrounds serve as a testbed for developing and validating object reconstruction, event selection, and calibration procedures within the `Easyjet` framework[3]. We focus on three main background categories: diphoton plus jets ($\gamma\gamma$+jets), top quark pair production with associated diphotons ($t\bar{t}\gamma\gamma$), and electroweak diboson plus diphoton production ($V\gamma\gamma$, where $V = W, Z$)[4]. The production of photons in these processes arises through several mechanisms, as illustrated by their leading-order Feynman diagrams. In the $\gamma\gamma$+jets background, photons are predominantly produced via initial-state radiation (ISR) from incoming quarks

or gluons, as well as from final-state radiation (FSR) off outgoing partons. In $t\bar{t}\gamma\gamma$, genuine prompt photons can originate from top quark decay chains, particularly from radiation off top decay products, and from radiation associated with $W \to \ell\nu$ decays[5]. These diagrams also allow for diagrams with photons emitted from virtual or real intermediate bosons, enhancing their similarity to BSM diphoton signatures.

The $V\gamma\gamma$ processes, such as $W\gamma\gamma \to \ell\nu\gamma\gamma$ and $Z\gamma\gamma \to \ell\ell\gamma\gamma$, feature photons produced directly from gauge boson radiation or from radiation off the fermionic legs. These processes are especially relevant due to their final-state configurations involving genuine leptons and photons, which directly overlap with our signal region of interest. Collectively, these SM backgrounds provide a realistic environment to evaluate the performance of lepton and photon isolation criteria, test tau vetoes, and optimize event selection strategies. By using these samples to construct cutflows and kinematic distributions, we aim to ensure that the analysis is robust and scalable when simulated signal samples become available.

(a) ISR + FSR photon emission in $q\bar{q} \to t\bar{t}$.

(b) FSR photon emission in $gg \to t\bar{t}$.

Figure 2: Representative Feynman diagrams contributing to the $\gamma\gamma + 2\ell$ final state in $t\bar{t}\gamma\gamma$ production. (a) Initial-state radiation (ISR) from the quark leg and final-state radiation (FSR) from the $W^- \to \ell\bar{\nu}$ decay. (b) Gluon-gluon fusion with one photon radiated from the $\bar{t}$ line and another from the leptonically decaying W^- boson. These configurations are important irreducible backgrounds in resonance searches involving photons and leptons[**?**].

The event selections applied to the $\gamma\gamma + 1\ell, 0\tau$ and $\gamma\gamma + 2\ell, 0\tau$final states incorporates strict requirements on photon and lepton reconstructions to ensure signal-like quality while suppressing background contributions. Photon candidates must pass Loose identification and FixedCutLoose isolation working points, both of which have been extensively validated in ATLAS Run 2 using 2015–2017 data [6, 7]. The identification criteria rely on shower shape variables and calorimeter cluster information, while isolation selections suppress contributions from nearby hadronic activity. As reflected in Table 1, approximately 76% of the events in the $t\bar{t}\gamma\gamma$ sample pass the photon ID and isolation criteria, in line with reported efficiencies for photon transverse momenta above 25–35 GeV and $|\eta| < 2.37$.

Lepton selection targets prompt electrons and muons from electroweak decays. Electrons are reconstructed using calorimeter and tracking information, passing the MediumLH identification and Loose isolation criteria defined by ATLAS [6], while muons pass Medium identification and Loose isolation requirements as defined in [8]. These criteria are designed to balance high reconstruction efficiency and fake rate suppression. The table shows that after lepton selection, about 73% of the events are retained. This drop is consistent with expectations, given that in the $t\bar{t}\gamma\gamma$ sample, leptons originate from W decays and must satisfy both kinematic and isolation thresholds. The final selection step imposes the 0-τ requirement and confirms the presence of one or two high-quality leptons. The cumulative efficiency sharply decreases to 3.6% in the $\gamma\gamma + 2\ell$ channel and to 38% in the $\gamma\gamma + 1\ell$ channel, reflecting both the branching fractions of the top decay and the stringent object-level selections described above.

3 Results

The results presented in this section are entirely based on Standard-Model background simulations, as signal Monte Carlo samples are currently in production and not yet available. We focus on the kinematic properties of photons and leptons in the $\gamma\gamma + 1\ell$, 0-τ and $\gamma\gamma + 2\ell$, 0-τ final states, currently using the $t\bar{t}\gamma\gamma$ sample as representative background. This sample allows us to study the characteristic distributions of key observables such as photon transverse momenta, diphoton invariant mass, lepton kinematics, angular separations, and missing transverse energy. While these distributions do not yet include contributions from potential BSM signals, they form the baseline for selection tuning and shape analysis. The insights gained here will inform future signal-region optimization and cut-based or multivariate strategies once signal samples are available.

Table 1: Cutflow comparison for the $\gamma\gamma+1\ell$ and $\gamma\gamma+2\ell$ final states using simulated $t\bar{t}\gamma\gamma$ events. The table shows the number of events passing each selection step and the corresponding relative efficiency, normalized to the total number of events.

Cut Description	$\gamma\gamma+1\ell$		$\gamma\gamma+2\ell$	
	Events Passed	**Efficiency**	**Events Passed**	**Efficiency**
Total events	534144	1.0	534144	1.0
Pass Photon ID and Isolation	405764	0.76	405764	0.76
Pass Photon Selections	405558	0.74	405558	0.74
Pass Lepton Selections	392068	0.73	392068	0.73
Final Selection (1ℓ or $2\ell+0\tau$)	201682	0.38	19028	0.036

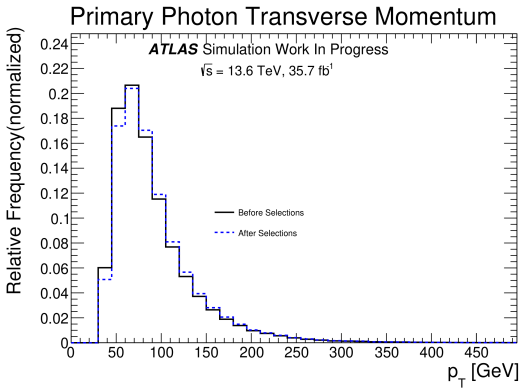

(a) Lead photon p_T

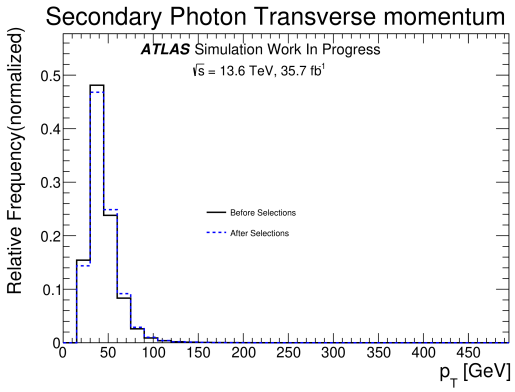

(b) Sublead photon p_T

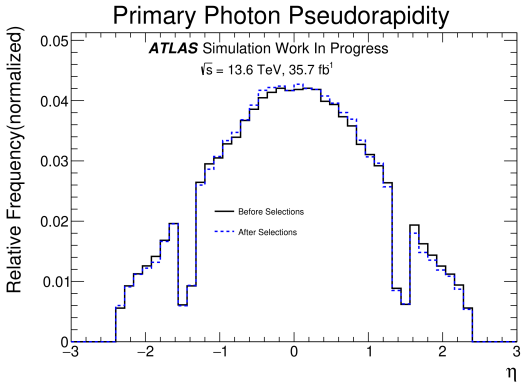

(c) Lead photon η

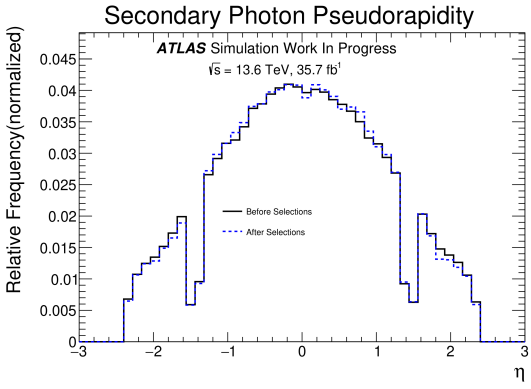

(d) Sublead photon η

Figure 3: Photon kinematic distributions for the above-mentioned $\gamma\gamma+leptons$, 0-τ final state. Top row: transverse momentum distributions show thresholds at $p_T = 35$ GeV (leading) and 25 GeV (subleading) due to event selection. Middle row: pseudorapidity distributions reveal dips around $|\eta| \approx 1.5$, corresponding to the calorimeter transition region[**?**] excluded by selection. These distributions are derived from the $tt\bar{\gamma}\gamma$ Ntuple sample used.

3.1 *Object kinematics:* $\gamma\gamma + 1\ell, 0\tau$ *Using the* $t\bar{t}\gamma\gamma$

We begin by looking at object-level selection, by exploring our photon-object kinematics from the $t\bar{t}\gamma\gamma$ Ntuple, looking at the transverse momentum and pseudorapidity.

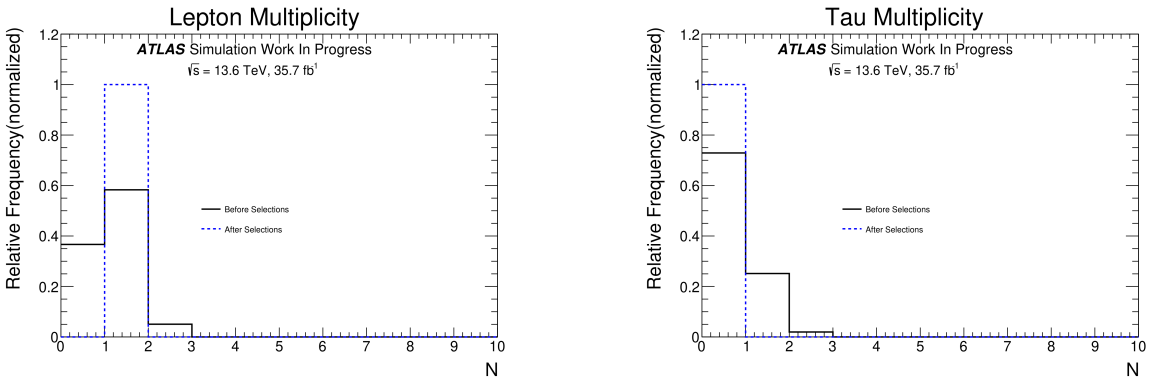

(a) Total lepton count per event.

(b) Tau multiplicity per event.

Figure 4: Total lepton and tau multiplicity distributions before and after selection. The lepton count plot confirms the selection's focus on $\gamma\gamma + 1\ell, 0\tau$ final state. The tau distribution shows a sharp suppression after selection, indicating that the 0-τ veto is functioning effectively to exclude events containing hadronically decaying tau candidates.

3.2 *Object kinematics:* $\gamma\gamma + 2\ell, 0\tau$ *Using the* $t\bar{t}\gamma\gamma$

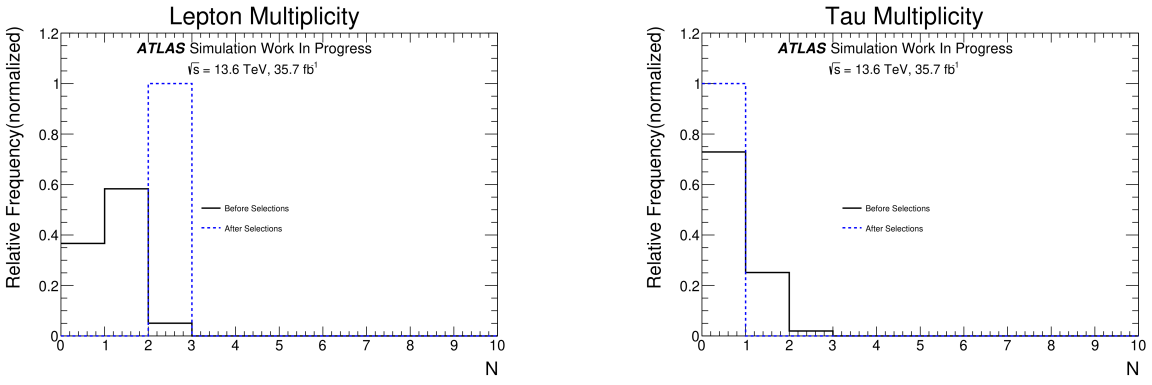

(a) Total lepton multiplicity per event.

(b) Tau multiplicity per event.

Figure 5: Lepton and tau multiplicity distributions before and after event selection for the $\gamma\gamma + 2\ell, 0\tau$ final state. Panel (a) shows a sharp concentration at two leptons after selection, matching the signal topology. Panel (b) confirms effective suppression of events containing tau candidates, validating the 0-τ requirement. The small residual tau presence before selection is removed by applying hadronic tau vetoes.

4 Conclusion

This study presents the development and validation of an event selection strategy for diphoton final states in the $\gamma\gamma + 1\ell, 0\tau$ and $\gamma\gamma + 2\ell, 0\tau$ channels, targeting scalar resonance decays predicted by models such as 2HDM+S. Using the $t\bar{t}\gamma\gamma$ background sample, we established baseline distributions and evaluated kinematic properties of photons and leptons under ATLAS Run 3-like conditions. Our analysis applied strict selection criteria based on

established ATLAS identification and isolation recommendations for photons, electrons, and muons, achieving efficient suppression of hadronic tau contamination as confirmed by tau multiplicity distributions.

The object-level studies demonstrated the effectiveness of the implemented selections in shaping signal-like topologies from background-rich samples. Lepton and tau multiplicities, as well as photon kinematic distributions, all reflect the designed event categories, validating our initial strategy. These distributions serve as reference benchmarks for later inclusion of signal Monte Carlo, which is currently in production.

Furthermore, the EasyJet framework provided a modular and reproducible infrastructure for this preparatory study, allowing rapid testing and refinement of cuts. The insights gained here are essential for optimizing future analyses targeting new physics in diphoton and multilepton final states. Once signal samples are incorporated, we will extend this work toward sensitivity studies and potential resonance reconstruction, contributing to the broader ATLAS BSM search program during Run 3.

References

[1] S. von Buddenbrock, A. S. Cornell, E. D. R. Iarilala, M. Kumar, B. Mellado, X. Ruan, and E. M. Shrif, "Constraints on a 2hdm with a singlet scalar and implications in the search for heavy bosons at the lhc," *Journal of Physics G: Nuclear and Particle Physics*, vol. 46, no. 11, p. 115001, Sep. 2019. [Online]. Available: http://dx.doi.org/10.1088/1361-6471/ab3cf6

[2] S. Ashanujjaman, S. Banik, G. Coloretti, A. Crivellin, S. P. Maharathy, and B. Mellado, "Anatomy of the real Higgs triplet model," *JHEP*, vol. 04, p. 003, 2025.

[3] Easyjet Collaboration, "Easyjet framework," https://gitlab.cern.ch/easyjet/easyjet, 2024, accessed: July 2025.

[4] ATLAS Collaboration, "Measurement of $Z\gamma\gamma$ production in pp collisions at $\sqrt{s} = 13$TeV with the ATLAS detector," *Eur. Phys. J. C*, 2023, arXiv:2211.14171.

[5] ATLAS Collaboration, "Observation of $t\bar{t}\gamma\gamma$ production at $\sqrt{s} = 13$ tev with the atlas detector," *arXiv e-Print*, vol. arXiv:2506.05018, 2025. [Online]. Available: https://arxiv.org/abs/2506.05018

[6] ATLAS Collaboration, "Electron reconstruction and identification in the ATLAS experiment using the 2015 and 2016 LHC proton–proton collision data at $\sqrt{s} = 13$ tev," *The European Physical Journal C*, vol. 79, no. 8, 2019. [Online]. Available: http://dx.doi.org/10.1140/epjc/s10052-019-7140-6

[7] ATLAS COLLABORATION, "Electron and photon efficiencies in lhc run 2 with the atlas experiment," *JHEP*, vol. 2024, no. 5, 2024. [Online]. Available: https://doi.org/10.1007/JHEP05(2024)162

[8] ATLAS Collaboration, "Muon reconstruction and identification efficiency in atlas using the full run 2 pp collision data set at $\sqrt{s} = 13$ tev," *The European Physical Journal C*, vol. 81, no. 7, 2021. [Online]. Available: http://dx.doi.org/10.1140/epjc/s10052-021-09233-2